

COB-2023-1787

ELECTROCHEMICAL ANALYSIS OF A MEMBRANELESS ELECTROLYZER FOR GREEN HYDROGEN PRODUCTION

Emerson Barbosa dos Anjos
Bruno Scaramuzza dos Reis
Samara da Silva Garcia
Caio Mayron de Carvalho Farolfe
Diego Busson de Moraes
Carolina Palma Naveira Cotta

Laboratory of Nano & Microfluidics and Micro-Systems – LabMEMS, UFRJ, Mechanical Eng. Dept., Federal.

emersonbanjos@ mecanica.coppe.ufrj.br
brunoscamuzza@mecanica.coppe.ufrj.br
samarasilvagarcia.20231@poli.ufrj.br
caiofarolfe@poli.ufrj.br
bussonn@gmail.com
carolina@mecanica.coppe.ufrj.br

Abstract. *With the increasing world population and the need to produce energy and fuels in a green way, several countries are searching for ways to decarbonize the energy matrix to ensure a sustainable future. In this sense, hydrogen is an alternative to this demand, known as the fuel of the future, due to its ability to store energy and its low molecular weight. However, the hydrogen produced today is mainly (94%) by steam reforming methane, which commonly natural gas is the feedstock. i.e. it is not a renewable process, compromising the decarbonization mission. Thus, an alternative for clean hydrogen production is water electrolysis, which can be coupled with renewable technologies such as hydropower, solar, or wind power. Among existing electrolyzers for hydrogen production, currently, the main one is the Proton Exchange Membrane (PEM) electrolyzer, however, the membrane has some disadvantages, including the need for a rather complex membrane electrode assembly architecture and the risk of device failure due to membrane fouling or degradation in the presence of impurities. As alternatives to the conventional PEM, there is interest in developing electrolysis architectures for which there are no membrane dividers positioned between the O₂ and H₂ evolution electrodes. These are known as membraneless electrolyzers and generally rely on product flow separation, where forced flow (advection) forces are used to guide the O₂ and H₂ products before they can cross to the opposite electrode. Thus, the present work aims to experimentally investigate the electrochemistry behavior of membraneless electrolytes in different electrolyte solutions (KOH, NaOH), electrodes (stainless steel mesh, carbon, and platinum titanium), and flow rate (0, 100, 200 ml/min). For the results, the current-voltage characteristic curves were measured by applying a varying potential to the working electrode over time, measuring the current generated in the solution, and the efficiency and specific energy consumption in each scenario. Thus, the present work has shown that this electrolyzer has enormous potential to meet society's clean and efficient fuel generation needs.*

Keywords: *Green Hydrogen, Membraneless, Electrolyzer.*

1. INTRODUCTION

Hydrogen, as a versatile and clean energy carrier, has garnered significant attention in recent years as a potential solution to mitigate climate change and address the challenges associated with fossil fuel depletion. Water electrolysis, the process of using an electric current to split water molecules into hydrogen and oxygen, has emerged as a prominent method for hydrogen production, since the 19th century (Santos et al., 2013). Electrolysis can be achieved using various types of electrolyzers, including membrane-based and membraneless electrolyzers, to produce hydrogen by cost-effective electrolysis and be a competitive technology compared to steam reforming, which comprises 94% of world production of hydrogen (Chen et al., 2020), but it is not a renewable process, since its main feedstock is natural gas, which means that this hydrogen is not within the limits of envisaged environmental policies.

The main commercial electrolyzers utilized in water electrolysis employ a solid polymer electrolyte membrane, enabling the selective transport of protons while preventing the mixing of hydrogen and oxygen gases (Esposito 2017). However, these membrane-based electrolysis face limitations such as high costs, durability issues, and performance degradation over time. To overcome these challenges, membrane-free electrolysis, also known as membraneless or membrane-free electrolyzers, has emerged as a promising alternative (Oruc et al., 2016; Esposito 2017; Rajora and Haverkort 2022).

A membraneless electrolyzer is an electrolysis system that operates without a physical membrane separating the electrodes. In a membraneless electrolyzer, the electrolyte solution acts as both the conductive medium and the means of separating the electrodes, allowing for direct contact between them (Yang et al., 2021; Yan et al., 2021). This design offers several advantages, including simplified system configuration, reduced cost, and enhanced flexibility in working with different electrolyte solutions (Pang et al., 2020). One notable phenomenon associated with membraneless electrolyzers is the Segré-Silberberg effect. This effect is a velocity-dependent phenomenon and that ensures that the generated bubbles are close to the wall of the electrolyzer (De et al., 2020). So, it guarantees the removal of the membrane, it is an efficient electrolyzer with a low cross-over (low mixture between H₂ and O₂ gases at the electrolyzer outlet). Regarding the main disadvantages today of the electrolyzer without a membrane are the purity of the product and security. Thanks to the ability of solid electrolyte membranes to serve as a physical barrier to O₂ and H₂ gases, commercial PEM electrolyzers can generate H₂ with high purity, typically 99.99%, while simultaneously compressing H₂ to pressures up to 150 bar, and membraneless electrolyzers cannot compress H₂ electrochemically because they are not capable of maintaining a significant pressure difference between the electrodes (Esposito, 2017).

The membraneless electrolyzer exhibits remarkable versatility in working with different electrolyte solutions. It can effectively operate with various electrolytes, including salt water, acidic media, and basic media (Talabi et al., 2017; Hashemi et al., 2015). This versatility enables the electrolyzer to adapt to different applications and tailor its performance to specific requirements. For example, it can utilize salt water as an electrolyte for on-site seawater electrolysis, enabling the direct production of hydrogen from abundant seawater resources and it can also operate in acidic or basic solutions, such as sulfuric acid or alkaline solutions, respectively, facilitating the generation of hydrogen in various industrial processes (Liang et al., 2023; Samir De et al., 2023; Hashemi et al., 2019).

In the literature, several studies have highlighted the importance of membraneless electrolyzers. For example, O'Neil et al., (2016), was one of the first papers published on membraneless electrolyzers for hydrogen production. The authors analyzed these electrolyzers for a 3D-printed electrolyzer with a body made of PLA and ABS materials. They examined the efficiency of the electrolyzers in different electrolyte solutions (1.0 M NaSO₂, 0.5M H₂SO₄, and 1.0M KOH), reporting their respective efficiencies (NaSO₂ = 49.7%, H₂SO₄ = 67.3%, KOH = 81.3% at 50mA/cm²), the authors detailed how simple a membraneless electrolyzer is (just a body, anode, and cathode) and briefly presented the possibility of modulating this equipment. Davis et al., (2019) investigated bubble dynamics in a membraneless electrolyzer using a high-speed camera, employing the same fabrication process as presented by O'Neil et al., (2016). The authors observed that larger bubbles were generated at higher current densities, since it is providing more energy for the reaction to occur, so, more gas is produced, and the larger the bubbles are close to the electrode. In addition, with a high-speed camera image, the authors have enabled the determination of the void fraction of bubbles at the end of the electrolyzer channel, important information to be able to improve the electrolyzer efficiency. Hadikhani et al., (2021) also analyzed the influence of bubbles in the electrolyzer channel, comparing different current densities and confirming, that larger bubbles are generated at high current densities, potentially affecting the efficiency of these electrolyzers. Furthermore, Hadikhani et al., (2021) suggested that for higher flow rates, smaller bubbles are generated, indicating an optimal flow rate for the equipment, and the addition of surfactant like PFOS can reduce bubble size, ensuring proper electrolyzer operation. However, in the literature, there is a lack of studies comparing the efficiency of this membraneless electrolyzer with different types of electrolyzers and directly comparing it with other commercial electrolyzers, such as PEM electrolyzers.

Thus, the present paper aimed to fabricate a membraneless electrolyzer and experimentally analyze its electrochemical performance in different alkaline electrolyte solutions (KOH and NaOH) using various electrodes (stainless steel, carbon electrode, and platinumized titanium). Additionally, the electrolyte flow rate was varied to assess the efficiency of the electrolyzer in each configuration, as determined by polarization curves. The results were compared with those obtained from a PEM electrolyzer (Electrolyzer 65 (FuelCellStore), membrane: *Nafion*®, electrode: stainless-steel), demonstrating the efficiency of the fabricated membraneless electrolyzer. Allowing to analyze its versatility in working with different electrolyte solutions, which expands the range of available feedstocks, enabling the utilization of abundant and affordable resources. This contributes to the production of green hydrogen, which is derived from renewable energy sources and helps reduce carbon emissions.

2. METHODOLOGY

The present paper focuses on the fabrication and experimental analysis of a membraneless electrolyzer for water electrolysis (Eq. (1)). An electrolyzer is an electrochemical cell that primarily consists of three key elements: 1. the electrolyzer body, 2. the electrodes used, and 3. the electrolyte for this electrolyzer. Currently, the most used electrolyzers are PEM (Proton Exchange Membrane) electrolyzers, which employ a membrane that serves two main purposes: to act as a barrier to prevent crossover at the electrolyzers outlet and to function as a solid electrolyte (Figure 1a), providing the necessary conductivity for water molecule dissociation through the passage of current (Eq. (1)). However, as mentioned earlier in this work, the membrane in these electrolyzers carries a high cost, and its removal presents an alternative to make the generated hydrogen price more competitive. In this regard, a membraneless electrolyzer (Figure 1b) becomes an option to lower the cost of this equipment. A membraneless electrolyzer operates with a liquid electrolyte (which can

be highly conductive water or an acidic/basic medium), which works without a barrier (membrane/diaphragm) between the electrodes and with an operational flow rate for the flow of the electrolyte solution.

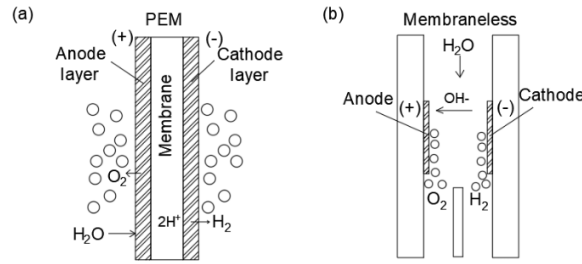
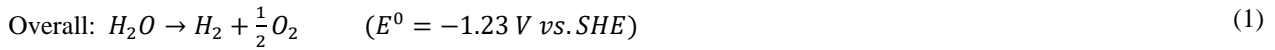


Figure 1. Simplified Schematics of Electrolyzer Technologies, (a) PEM, (b) Membraneless.

The overall reaction of water electrolysis is given in Eq. (1), generating hydrogen and oxygen as a product, and this hydrogen can be applied in fuel cells, for example.



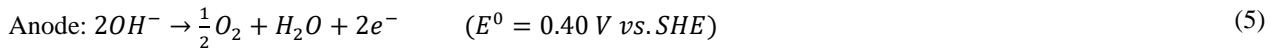
In the electrolyzer (PEM or ME), the electrodes for each configuration undergo two distinct half-cell reactions, where at the cathode, the Hydrogen Evolution Reaction (HER) occurs, and at the anode the Oxygen Evolution Reaction (OER) takes place.

In a PEM electrolyzer, the following reactions occur, Eq. (2) and Eq. (3):



Where SHE is Standard Hydrogen Electrode. In PEM, at the anode, water is oxidized, releasing molecular oxygen (O_2), protons (H^+), and electrons (e^-). These protons are then transported through the polymer membrane to the cathode. At the cathode, the protons are reduced, forming hydrogen molecules (H_2). The proton exchange membrane acts as an electronic insulator, allowing only the passage of protons while maintaining the separation of the anode and cathode half-cells. It also serves as an electrolyte to facilitate protonic conduction, avoiding having to add any substance to increase the conductivity of the water.

To the process in an alkaline electrolyte, in this case, the membraneless electrolyzer, the electrochemical reactions occurring at the cathode and anode are given by Eq. (4) and Eq. (5), respectively:



The calculation of these equations, Eq. (4-5) and Eq. (2-3), (the potential of an electrochemical cell to water electrolysis is calculated by the difference between the potential of the cathode and anode) will lead to the same overall potential as described in Eq. (1), with the same value (-1.23 V) for the theoretical cell voltage. At the cathode, the reduction of the water occurs, resulting in the formation of hydroxide ions (OH^-), and hydrogen (H_2). These hydroxide ions are transported through the alkaline electrolyte solution to the anode. At the anode, the hydroxide ions are oxidized, forming oxygen (O_2) and water (H_2O).

Unlike a membrane-based electrolyzer, the alkaline membraneless electrolyzer does not require a physical barrier to separate the half-cells, as the alkaline electrolyte solution serves as the conductor for the hydroxide ions between the anode and cathode. Additionally, the electrodes are typically made of porous materials such as nickel, stainless steel, or titanium screen, which allow for the passage of ions and facilitate electrochemical reactions.

Moreover, to evaluate the electrochemical efficiency of an electrolyzer and understand the sources of its efficiency losses, it is useful to consider the relationship between the electrolysis current (i), and the voltage (V) that is applied between the anode and cathode. The applied voltage is equal to the sum of the thermodynamically required voltage to split water ($\Delta E_{H_2O}^0 = 1.23$), and the voltages required to overcome kinetic (η_{HER} and η_{OER}), Ohmic (iR_s), and mass transport (η_{mt}) losses:

$$V = \Delta E_{H_2O}^0 + \eta_{HER} + \eta_{OER} + iR_s + \eta_{mt} \quad (6)$$

To achieve maximum electrolysis efficiency, the kinetic, mass transfer, and ohmic losses must be minimized. η_{HER} (cathode overvoltage) and η_{OER} (anode overvoltage) can be minimized by selecting efficient catalysts in the electrodes and using electrodes with high surface area, while “ iR_s ” (where R_s is the cell ohmic resistance) may be reduced by optimizing the cell geometry (for example, the channel in a membraneless electrolyzer and the gas diffusion plates in a PEM electrolyzer) and maximizing electrolyte conductivity. η_{mt} (mass transport overvoltage) can be minimized by using a high conductivity electrolyte (e.g. KOH) and employing forced convection of the electrolyte.

In this sense, calculating the efficiency of an electrolyzer is of paramount importance in assessing its performance and determining its energy consumption. The efficiency calculation is typically based on the Higher Heating Value (HHV) of hydrogen, which quantifies the energy content of the produced hydrogen gas. The HHV of hydrogen is commonly considered to be 1.48 V. Furthermore, The HHV is often used as a more realistic estimate of the energy efficiency in the electrolysis process, as the voltage from Eq. (3) of 1.23 V represents the minimum thermodynamic potential required for water electrolysis, known as the water reduction potential.

The electrochemical efficiency of the electrolyzer (ε), Eq. (7) is calculated by the ratio of the HHV by the voltage applied to the electrolyzer (Eq. (6)). This efficiency calculation provides valuable insights into the effectiveness of the electrolysis process in converting electrical energy into hydrogen energy.

Another key aspect in evaluating electrolyzer efficiency is the calculation of specific energy consumption (SEC) using Faraday's law. The SEC calculation takes into account the current flowing through the electrolyzer, the current efficiency, and the voltage applied to the electrolyzer, according to Eq. (8).

$$\varepsilon = \frac{HHV}{V} \quad (7) \quad SEC = \frac{V i t}{E_c} \quad (8)$$

Where E_c is the current efficiency (it is calculated by Faraday's law, with a frequent value of 90-100% in electrochemical cells (West, 2013)). The ε and SEC calculations enable researchers and industry professionals to assess the performance of electrolyzers, optimize their operation, and compare different electrolyzer designs and technologies. This information aids in the development of more efficient and cost-effective hydrogen production systems, facilitating the transition towards sustainable and green energy solutions.

By understanding and analyzing efficiency and SEC, researchers can make informed decisions about the selection, design, and operation of electrolyzers, contributing to the advancement of hydrogen technologies and the realization of a clean and sustainable energy future. In this sense, the present study was designed to compare these performance parameters of a membraneless electrolyzer and a PEM, to guide the evolution of the proposed technology.

2.1 Device Fabrication and Electrode Information

The body of the membraneless electrolyzer (Fig 2a) was made of acrylic using a laser machine for cutting and engraving (Gravograph LS100). This body is divided into three parts (Figure 2b, expanded view (in CAD) of a membraneless electrolyzer), measuring 90 x 35 mm. The upper part (Figure 2c) serves as the electrolyzer lid, with 8 holes for countersunk screws (M3 x 0.5 x 15), three M5 threaded holes for inserting a 4 mm hose pipe connector (push connect fittings), one for the electrolyte inlet, and two outlets - one for hydrogen and electrolyte solution, and the other for oxygen and electrolyte solution. The lid also includes a region for accommodating an O-Ring for electrolyzer sealing. The middle part (Figure 2d) comprises the electrolyzer channel, with a height of 5mm, length of 42mm, and width of 7mm, through which the electrolyte solution flows and where the electrodes are placed to facilitate the reactions represented by Eq. (2) and Eq. (3). In this central part, a downstream partition is added to ensure there is no gas mixing at the equipment outlet. The lower part of the electrolyzer (Figure 2e) features eight M3 threaded holes for screw fastening and a region for inserting an O-Ring, ensuring proper equipment sealing.

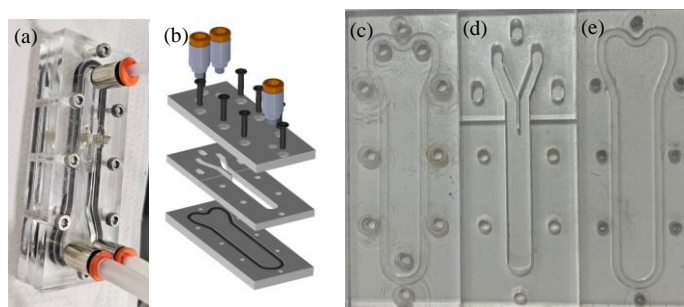


Figure 2. (a) Membraneless Electrolyzer, (b) Expanded view (in CAD) of a membraneless electrolyzer, (d-f) Part in acrylic representing the body of the membraneless electrolyzer.

For the electrodes, three commercial configurations were adopted in this work. These include a platinumized titanium mesh (80-mesh count, FuelCellStore), a carbon cloth with the following specifications: 0.03 mg/cm² 20% Platinum on Vulcan-Carbon Cloth Electrode, (FuelCellStore), and a stainless-steel mesh with a 120-mesh count (Telasa/RJ). With these electrode configurations, the electrolyzer is assembled and ready for experimental measurements using the desired electrolytic solution (KOH or NaOH).

2.2 PEM Electrolyzer and Membraneless Electrolyzer: Experimental Apparatus

The experimental setup for the PEM electrolyzer involves the use of the Electrolyzer 65 (FuelCellStore). This advanced system consists of a two-cell electrolysis stack, accompanied by a hydrogen storage tank and an oxygen storage tank, all securely mounted on a sturdy baseplate. The two individual cells within the electrolysis stack are electrically interconnected in series, facilitating efficient operation. In addition, the PEM electrolyzer in each cell has electrodes with an area of 16cm², stainless steel, and Nafion[®] membrane.

Located at the center of the electrolysis stack, the hydrogen side of the two cells is responsible for the generation and collection of hydrogen gas. The outer sides of the stack are dedicated to the supply of distilled water as an electrolyte and the removal of the produced oxygen gas. This process is facilitated through the use of tubes, allowing for the controlled extraction of hydrogen and oxygen gases from their respective compartments.

To ensure proper electrical connections, the electrolysis stack is equipped with two 4 mm female connectors that enable seamless plug integration. These connectors play a crucial role in establishing reliable electrical pathways within the system, promoting stable and consistent electrolysis performance. The well-designed configuration of the Electrolyzer 65 offers a robust and versatile setup for conducting PEM electrolysis experiments with precise control over hydrogen and oxygen gas generation. For the PEM electrolyzer was used deionized water with a conductivity lower than 0.05×10^{-6} S/cm.



Figure 3. Experimental setup of the commercial PEM electrolyzer bench.

The experimental setup for the Membraneless Electrolyzer (ME) involves some key components (Figure 4a). Firstly, an LDP-301-11 (MS TECNOPON) peristaltic pump is utilized to circulate the electrolytic solution (1M KOH or 1M NaOH solutions, with deionized water of conductivity lower than 0.05×10^{-6} S/cm) from “Tank 1” to the ME setup. The electrolytic solution, along with the resulting reaction products, is directed to the “Tank 2” (with 4mm PTFE tubes), where the gases can be efficiently separated for different applications (*e.g.* fuel cell), (Figure 4b).

To control and monitor the electrolyzers operation, a PS-5000 (0-32V and 3A, ICEL Manaus) power supply is employed. This power supply provides the necessary voltage to the electrolyzer while allowing for the monitoring of hydrogen production, flow rate effects, and bubble generation within the electrolyzer. Precise control of these parameters ensures accurate data collection and analysis.

To measure the performance of the electrolyzer, a Fuel Cell Monitor Pro (FuelCellStore) is used. This device functions as a voltage controller, gradually supplying a range of voltages (0-4V) to the electrolyzer while continuously monitoring the current passing through it. The collected voltage and current data are then processed using specialized software provided by the Fuel Cell Monitor Pro, allowing for the generation of polarization curves for different configurations. These curves provide essential insights into the electrolyzers efficiency and performance under varying conditions.

By employing this experimental setup, the membraneless electrolyzers efficiency can be assessed. The setup allows for the investigation of various factors, including different electrolyte concentrations, flow rates, and electrode materials, to evaluate their impact on the electrolyzers performance. The data obtained, along with the generated polarization curves, offer valuable insights into the electrolyzers suitability for hydrogen generation across diverse applications.

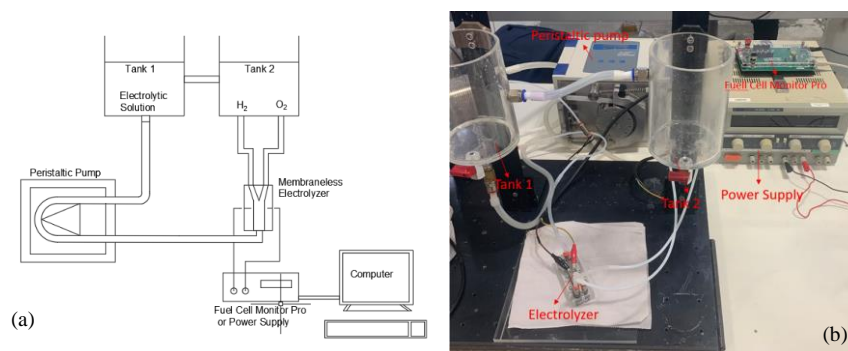


Figure 4. (a) schematic diagram of the experimental setup (b) Experimental setup of the membraneless electrolyzer bench.

3. RESULTS

In this study, the results were analyzed using a polarization curve for Membraneless Electrolyzer (ME) with three different pairs of electrodes: Vulcan-Carbon Cloth, platinized titanium, and stainless steel, all with an area of 0.6 cm^2 , in electrolytic solution of 1.0 M KOH or 1.0 M NaOH , and these results were compared with the commercial PEM electrolyzer (Fuel Cell Store, stainless steel electrode, deionized water and *Nafion*® Membrane). The polarization curve is a characteristic curve that informs the current/voltage relationship of an electrochemical cell, based on the electrode material, electrolyte solution, and the electrolyzer configuration, with it is possible to determine a current value, and so, identify the electrolyzer voltage and apply Eqs. (6, 7, and 8) to calculate the losses, the efficiency of the electrochemical cell, and the Specific Energy Consumption (SEC). Furthermore, this study also investigated the influence of different flow rates (200, 100, and 0 ml/min) on the electrolyzers performance. By varying the flow rate, it is possible to evaluate its impact on the voltage-current density relationship and analyze the effect of bubbles on the electrolyzer. This analysis provided valuable information on the optimal flow rate for achieving high hydrogen production efficiency. Overall, the combination of polarization curves with electrode and flow rate variations offered a comprehensive understanding of the electrolyzers performance under different conditions, aiding in the development of improved electrolysis systems for hydrogen production.

In this way, Figure 5, shows a polarization curve that was obtained for a Membraneless Electrolyzer (ME) with platinized titanium electrode (Figure 5a) and stainless steel (Figure 5b) with an electrolytic solution of 1.0 M KOH (blue curve) and 1.0 M NaOH (black curve), in addition, a comparison with the polarization curve for PEM electrolyzer was also performed. In Figure 5, the polarization curve was analyzed with voltage ranging from 0 to 4 V , due to the limitation of the equipment used (Fuel Cell Monitor Pro), and for current density, it was limited to 200 mA/cm^2 , which presents all possible measurements for a PEM electrolyzer (since the maximum current density obtained was 167 mA/cm^2 at a voltage of 4 V).

For the comparison of electrolyte solutions (KOH or NaOH) in a platinized titanium electrode (Figure 5a), it is possible to observe that for both solutions the increase of the voltage applied in the ME there is an increase in the current density, showing a typical behavior of polarization curve in ME. In Eq. (1) is given that water electrolysis has a minimum voltage equal to 1.23 V , however at 1.23 V (dashed red line), it is observed in Figure 5a that the current density in all cases (ME-KOH, ME-NaOH, and PEM) are equal to zero, indicating that no reaction occurs, so losses happen, as shown in Eq. (6). Thus, to analyze these losses it is necessary to define a constant value of current density and identify which voltage is obtained in this current density, the difference of the value obtained with 1.23 is precisely the kinetic, ohmic and mass transport losses identified in Eq. 6. In this way, a current density of 150 mA/cm^2 was arbitrarily adopted, these current density values are represented by points, where P1 refers to the point to the ME with platinized titanium electrode and KOH electrolyte solution, whereas P2 the same electrolyzer, but with NaOH as electrolyte solution, and P3 to the PEM electrolyzers. It is possible to observe that the losses of 1.74 V for the KOH solution are lower than those with the NaOH solution (2.22 V), through the Fuel Cell Monitor Pro (equipment used for measuring data), it is not possible to identify the contribution of each loss separately, but commercially alkaline electrolyzers use KOH as electrolyte because it presents a greater conductivity compared to NaOH (Santos et al., 2013), and in this case, the advantage of using KOH was confirmed. In addition, it was compared with the PEM electrolyzer, and it can be seen that the losses in the PEM are totaling 2.71 V , much higher than the solution with KOH or NaOH , although it is not possible to confirm each loss individually on the equipment, through the literature it is possible to state that the presence of *Nafion*® membranes introduces additional resistance to ion transfer, leading to ohmic losses during the electrolysis process (Esposito, 2017; Hodges et al., 2022). The membrane acts as a barrier that hinders the movement of ions, increasing the overall electrical resistance and reducing efficiency, so the main factor that confirms the higher efficiency of membraneless electrolyzers compared to PEM electrolyzers is the absence of a membrane. This key design feature allows for a reduction in energy losses associated with ion transport and lowers ionic resistance.

Continuing the comparison, Figure 5b shows the polarization curve for a membraneless electrolyzer with a stainless-steel electrode and with two different electrolyte solutions of 1.0 M KOH (blue curve) and 1.0 M NaOH (black curve), these results are compared again with a commercial PEM electrolyzer (orange curve). By examining the polarization curves of the stainless-steel electrode with NaOH (black curve) and KOH (blue curve) solutions, the voltage-current density relationship for that electrode is evaluated. As in Figure 5a, the absolute losses were calculated for the membraneless electrolyzer and with stainless steel electrode at 150 mA/cm² (where P4 = 2.86 V (1.23 + 1.63) that indicates voltage value to the membraneless electrolyzer with KOH to 150 mA/cm², P5 = 3.45 V (1.23 + 2.22V) the voltage value to the membraneless electrolyzer with NaOH, and P6 = 3.94 V (1.23 + 2.71 V) voltage value to the commercial PEM electrolyzer), it was once again seen that the KOH solution presents fewer losses, than NaOH solution and once again the membraneless electrolyzer is electrochemically more efficient than the commercial PEM electrolyzer (P4 < P5 < P6).

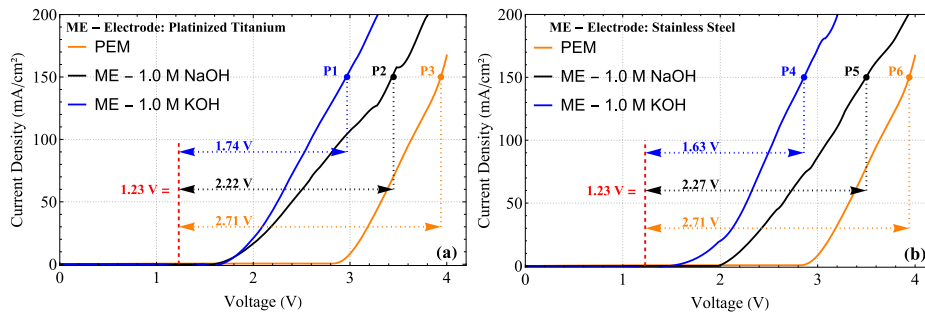


Figure 5. Polarization curve comparing Membraneless Electrolyzers (ME) with NaOH and KOH electrolytic solution (with flow rate = 200 ml/min) on different electrodes (a) platinumized titanium and (b) stainless steel, with a commercial PEM electrolyzer.

Figure 6a analyzes the polarization curve for the 0.03 mg/cm² 20% Platinum on the Vulcan-Carbon Cloth electrode. This electrode was chosen since carbon electrodes are very popular, because, unlike metallic electrodes, carbon is quite inert during electrolysis and therefore does not react with the solution. Analyzing the polarization curve, it is observed that the Vulcan-Carbon Cloth Electrode reaches a maximum current density of 58 mA/cm² at 4V, therefore having a much smaller range than that shown in Figure 5, this happens because the surface area to access the active site of the reactions is very small compared to a platinumized titanium mesh or stainless steel mesh, therefore it has lower current densities. To analyze the losses, a current density of 25 mA/cm² was considered, because above these the current density values are very similar for the two electrolytic solutions proposed in this paper (1.0 M NaOH, black curve, and 1.0 KOH, blue curve). Thus, points P7 (25 mA/cm² for ME - 1.0 M KOH) and P8 (25 mA/cm² for ME - 1.0 M NaOH) were obtained, showing that the losses in these two electrolytic solutions have very close values (1.68V and 1.67, respectively), identifying that the differences in ionic mobility between sodium (Na⁺) and potassium (K⁺) ions were not as relevant with an electrode of 0.03 mg/cm² 20% Platinum on Vulcan-Carbon Cloth Electrode, with current density of 25 mA/cm². In addition, to the commercial PEM electrolyzer, P9 represents the point with a current density of 25 mA/cm² and voltage of 2.52, therefore, greater losses were obtained, so, a ME with Carbon Electrode is more efficient. However, in Figure 6a, point P10 is displayed, to indicate that for current densities greater than 32 mA/cm² or voltage greater than 3.2, the efficiency of the PEM electrolyzer is better than ME with carbon cloth, showing that the kinetic and mass transport losses will be very relevant in the membraneless electrolyzer (since, as this electrolyzer has no barrier, the ohmic resistance is reduced, (Hodges et al., 2022)) with a carbon cloth electrode.

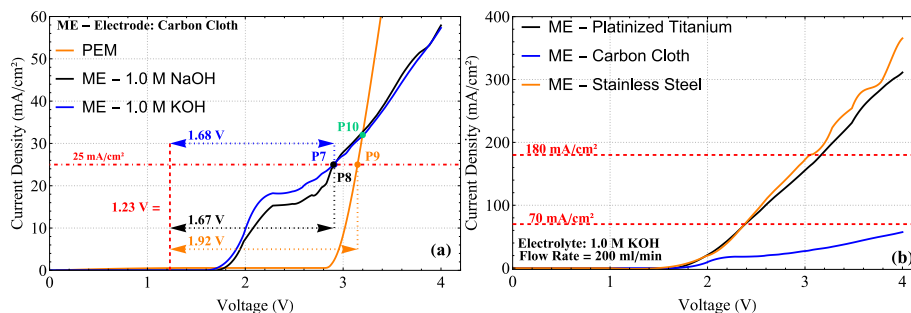


Figure 6. (a) Polarization curve comparing Membraneless Electrolyzers (ME) with NaOH and KOH electrolytic solution on the electrode with 0.03 mg/cm² 20% Platinum on Vulcan-Carbon Cloth and flow rate = 200 ml/min, with a commercial PEM electrolyzer and (b) Polarization curve for different electrodes in the membraneless electrolyzer.

Figure 6b shows the polarization curve for the ME with the following electrodes: platinized titanium mesh (black curve), the carbon cloth electrode (blue curve), the stainless-steel mesh (green curve) showing the maximum values of current density obtained at a voltage of 4V and with the electrolyte solution of 1.0M KOH (KOH was chosen because it is the most used in commercial models of alkaline electrolyzers, Santos et al., (2013) and Esposito (2017)) and has fewer losses than NaOH, thus being the most suitable solution) with a flow rate of 200 ml/min. When comparing the polarization curves of the platinized titanium electrode (mesh with open area = 57%), stainless-steel electrode (mesh, with open area = 49%), and carbon electrode (cloth), it is possible to see that for low current densities ($< 70 \text{ mA/cm}^2$) the stainless steel and platinized titanium electrodes have very similar behavior, while the carbon cloth electrode needs higher voltage values to reach the same currents, reaching its maximum current value at approximately 58 mA/cm^2 , as commented in Figure 6a. For higher current densities ($> 70 \text{ mA/cm}^2$) a small advantage is seen for stainless steel electrodes since they need a lower voltage for the same current density. However, a notable distinction arises at current density $> 180.0 \text{ mA/cm}^2$ specifically with the stainless-steel electrode. In this range ($> 180.0 \text{ mA/cm}^2$), can observe an irregularity in the polarization curve that is mainly in the stainless-steel electrode. The presence of this irregularity in the polarization curve of the stainless-steel electrode is probably due to factors such as uneven reactant distribution, localized concentration variations, and the accumulation of gas bubbles at the electrode surface, as discussed by O'Neil, et al., (2016).

At high current densities, the stainless-steel electrode may experience limitations in mass transport (since this electrode has a lower exchange current density than platinized titanium electrodes, West (2013)), resulting in uneven distribution of reactants and reduced efficiency of the electrochemical reactions. These limitations can lead to the formation of gas bubbles and the depletion of reactants near the electrode surface. Consequently, these localized effects manifest as a wave behavior in the polarization curve. On the other hand, the platinized titanium electrode exhibits a more consistent behavior without the presence of these instabilities, since the generated bubbles easily detach from the platinized titanium electrode which does not happen in stainless steel. The presence of platinum catalyst on the titanium surface enhances its electrocatalytic activity, reducing mass transport limitations and promoting more uniform electrochemical reactions, even at high current densities. So, these observations highlight the importance of considering the electrode material when designing efficient and stable electrolyzers for high-current density applications.

In a membraneless electrolyzer, the flow of electrolytes plays a crucial role in guiding the bubbles along a specific path, ensuring continuous renewal of the electrolyte near the electrode surface. This phenomenon has a significant impact on the shape and behavior of the polarization curves and was seen in Figure 7, and a photograph of the bubbles and the possible problem is shown in Figure 8.

To investigate the effect of flow rates on the polarization curves, for membraneless electrolyzer, a comparison was conducted between platinized titanium (Figure 7a) and stainless steel (Figure 7b) electrodes. The results showed that at low flow rates (0 and 100 ml/min), the polarization curve exhibited numerous instabilities. This can be attributed to the insufficient removal of gas bubbles from the electrode surface (O'Neil, et al., (2016)), as observed in Figure 8a and 8b (to 0 and 100 ml/min), leading to uneven reactant distribution and localized concentration variations. These factors contribute to higher overpotentials and voltage fluctuations, resulting in the instabilities observed in the curve.

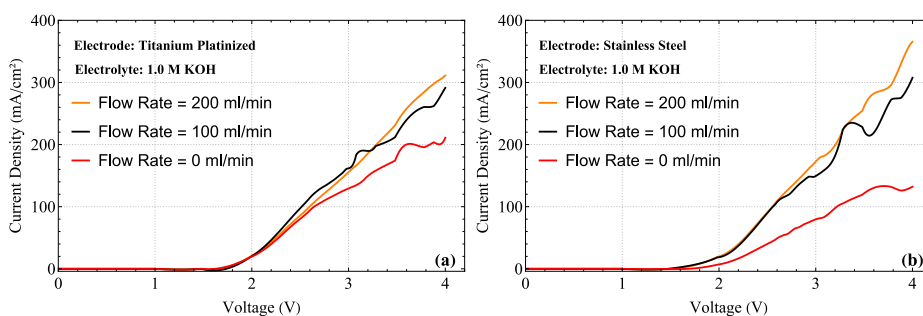


Figure 7. Polarization curve for the (a) platinized titanium and (b) stainless steel electrolyzer at different flow rates and with 1M NaOH solution.

On the other hand, as the flow rate of the electrolyte increased, the polarization curve became more "well-behaved" and smoother. The higher flow rate facilitated the efficient removal of gas bubbles from the electrode surface (Figure 8c to 200ml/min), ensuring a more uniform reactant distribution and minimizing localized concentration variations. Consequently, this led to a more stable and consistent behavior of the polarization curve.

In terms of the comparison between stainless steel and platinized titanium electrodes, stainless steel consistently exhibited a poorer performance in terms of instabilities in the polarization curve. This can be attributed to the lower catalytic activity and increased susceptibility to gas bubble accumulation of stainless steel compared to platinized titanium. The platinized titanium electrode, with its enhanced catalytic properties, tends to provide a more stable and regular polarization curve even under varying flow rates. Understanding the influence of flow rates and electrode materials

on the formation and removal of gas bubbles is crucial for optimizing electrolyzer performance. By selecting appropriate flow rates and utilizing suitable electrode materials, it is possible to minimize irregularities in the polarization curve, ensuring improved efficiency and stability of the electrolysis process.

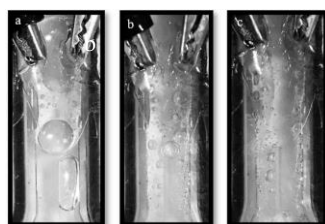


Figure 8. Photograph of the bubbles in the electrolyzer channel, for flow rates of (a) 0 ml/min, (b) 100 ml/min, and (c) 200 ml/min.

With the Eqs. (6, 7, and 8), the losses, efficiency (ϵ), and Specific Energy Consumption (SEC) of each electrolyzer configuration were calculated for a flow rate of 200 ml/min (because it is the one with the most stable polarization curve) and a comparison with a literature paper, are presented in Table (1). The membraneless electrolyzer demonstrates lower losses on all electrodes and higher efficiency compared to the PEM electrolyzer ($\epsilon = 47.74\%$), as discussed above, in Figures 5 and 6. In the case of a platinized titanium mesh electrode ($\epsilon = 66.1\%$), although the absolute value of efficiency is similar to that of stainless-steel mesh ($\epsilon = 65.7\%$), the hydrogen evolution reaction is more favorable with platinized titanium as electrode, as seen in the table of standard electrodes and by the exchange current density (that is more efficient on platinum and titanium electrodes than stainless steel, available in many electrochemistry books (*e.g* West, 2013)). The electrode with 0.03 mg/cm² 20% Platinum on Vulcan-Carbon Cloth, although displaying lower efficiency ($\epsilon = 39.2\%$), because of a lower specific surface area, presents the advantage of potential utilization in future designs featuring asymmetric electrodes (anode and cathode of different materials, Jiang et al., 2022), since inert carbon electrodes work well as anodes in electrochemical cells (West, 2013). Furthermore, when compared with work available in the literature (Mohammad et al., 2015), with membraneless electrolyzer and parallel electrodes, it is observed that the current work presents an efficiency close to that in the literature (this work, $\epsilon = 66.1\%$, literature $\epsilon = 67\%$), even working with a cheaper electrode. So, this configuration can enable unique applications and improved electrolysis performance by taking advantage of the distinct properties and catalytic activities of different electrode materials.

Table 1. Comparison of losses, efficiency, and energy consumption in different configurations of the electrolyzer and current density of 50 mA/cm².

	Electrolyzer	Electrode	Losses (V)	Efficiency (%)	SEC (kWh/kg)
This Work	PEM	Stainless Steel.	1.92	47.74	175.0
This Work	ME – KOH	Platinized Titanium	0.81	66.1%	113.3
This Work	ME – KOH	Stainless Steel	0.84	65.7%	115
This Work	ME – KOH	Vulcan Carbon Cloth	1.68	39.2%	161.67
Mohammad et al., (2015)	ME – H ₂ SO ₄	Platinum	0.97	67%	-

4. CONCLUSION

In conclusion, this study investigated the performance, losses, and irregularities in polarization curves of membraneless electrolyzers, and bubbles influence, specifically examining the influence of electrode materials and electrolyte flow rates. The findings underscore the significance of membraneless electrolyzers as an alternative to PEM electrolyzers for hydrogen production. The absence of a membrane in electrolyzers allows for the efficient removal of gas bubbles through optimal electrolyte flow, ensuring continuous renewal of the electrolyte near the electrode surface. Polarization curves exhibited irregularities at low flow rates, indicating localized concentration variations and inefficient reactant distribution, mainly due to the accumulation of bubbles in the channel, as can see in Figures 5, 6 and 7. Conversely, higher flow rates resulted in smoother and more stable polarization curves, indicative of enhanced efficiency.

Comparing electrode materials, platinized titanium consistently outperformed stainless steel and carbon cloth electrode, yielding more favorable polarization curves with fewer irregularities (Figure 7). The platinum catalysts on the titanium surface enhanced electrocatalytic activity, mitigating mass transport limitations and promoting uniform electrochemical reactions. The findings highlight the importance of electrode selection and flow rate optimization in membrane-free electrolyzers. Platinized titanium electrodes exhibit superior performance, underscoring their suitability for efficient hydrogen production. Moreover, electrolyte flow rate significantly influences bubble removal and reactant distribution (Figure 8), emphasizing the need for careful optimization to achieve optimal polarization curve behavior.

Membraneless electrolyzers offer advantages over PEM electrolyzers, such as simplified system design and reduced cost, mainly because it doesn't have a membrane to degrade. This study contributes valuable insights into membraneless

electrolyzer performance, aiding in their further development and optimization. These efforts will contribute to the advancement of sustainable and efficient hydrogen production technologies, fostering the transition towards a cleaner and more sustainable energy future.

5. ACKNOWLEDGEMENTS

The authors are indebted to the sponsoring agencies Capes and FAPERJ.

6. REFERENCES

- Chen, L., Qi, Z., Zhang, S., Su, J., and Somorjai, G. A. 2020. "Catalytic hydrogen production from methane: A review on recent progress and prospect". *Catalysts*, Vol. 10, n.8, p.858.
- Davis, J. T., Brown, D. E., Pang, X., and Esposito, D. V. 2019. "High speed video investigation of bubble dynamics and current density distributions in membraneless electrolyzers". *Journal of The Electrochemical Society*, Vol. 166, n. 4, p. F312.
- De, B. S., Singh, A., Dixit, R. J., Khare, N., Elias, A., and Basu, S. 2023. "Hydrogen generation in additively manufactured membraneless microfluidic electrolysis cell: Performance evaluation and accelerated stress testing". *Chemical Engineering Journal*, Vol. 452, p. 139433.
- De, B. S., Singh, A., Elias, A., Khare, N., and Basu, S. 2020. "An electrochemical neutralization energy-assisted membrane-less microfluidic reactor for water electrolysis". *Sustainable Energy & Fuels*, Vol. 4, n. 12, p. 6234-6244.
- Esposito, D. V. 2017. Membraneless electrolyzers for low-cost hydrogen production in a renewable energy future. *Joule*, Vol.1, n.4, p.651-658.
- Hadikhani, P., Hashemi, S. M. H., Schenk, S. A., and Psaltis, D. 2021. "A membrane-less electrolyzer with porous walls for high throughput and pure hydrogen production". *Sustainable energy & fuels*, Vol. 5, n. 9, p. 2419-2432.
- Hashemi, S. M. H., Karnakov, P., Hadikhani, P., Chinello, E., Litvinov, S., Moser, C., and Psaltis, D. 2019. "A versatile and membrane-less electrochemical reactor for the electrolysis of water and brine". *Energy & Environmental Science*, Vol. 12, n. 5, p. 1592-1604.
- Hashemi, S. M. H., Modestino, M. A., and Psaltis, D. 2015. "A membrane-less electrolyzer for hydrogen production across the pH scale". *Energy & Environmental Science*, Vol. 8, n. 7, p. 2003-2009.
- Hodges, A., Hoang, A. L., Tsekouras, G., Wagner, K., Lee, C. Y., Swiegers, G. F., and Wallace, G. G. 2022. A high-performance capillary-fed electrolysis cell promises more cost-competitive renewable hydrogen. *Nature communications*, Vol. 13, n. 1, p. 1304.
- Jiang, S., Ding, J., Wang, R., Deng, Y., Chen, F., Zhou, M., and Xu, C. 2022. "High performance NiCo-LDH/Fe₂O₃ asymmetric supercapacitors based on binder-free electrodes with dual conductive networks". *Chemical Engineering Journal*, Vol. 431, p. 133936.
- Liang, N. N., Han, D. S., and Park, H. 2023. "Membraneless unbuffered seawater electrolysis for pure hydrogen production using PtRuTiOx anode and MnOx cathode pairs". *Applied Catalysis B: Environmental*, Vol. 324, p. 122275.
- O'Neil, G. D., Christian, C. D., Brown, D. E., and Esposito, D. V. 2016. "Hydrogen production with a simple and scalable membraneless electrolyzer". *Journal of The Electrochemical Society*, Vol. 163, n. 11, p. F3012.
- Oruc, M. E., Desai, A. V., Nuzzo, R. G., and Kenis, P. J. 2016. "Design, fabrication, and characterization of a proposed microchannel water electrolyzer". *Journal of Power Sources*, 307, 122-128.
- Pang, X., Davis, J. T., Harvey, A. D., and Esposito, D. V. 2020. "Framework for evaluating the performance limits of membraneless electrolyzers". *Energy & Environmental Science*, Vol. 13, n.10, p.3663-3678.
- Rajora, A., and Haverkort, J. W. 2022. "An analytical multiphase flow model for parallel plate electrolyzers". *Chemical Engineering Science*, Vol. 260, p.117823.
- Santos, D. M., Sequeira, C. A., and Figueiredo, J. L. 2013. "Hydrogen production by alkaline water electrolysis". *Química Nova*, Vol.36, p.1176-1193.
- Talabi, O. O., Dorfi, A. E., O'Neil, G. D., & Esposito, D. V. 2017. "Membraneless electrolyzers for the simultaneous production of acid and base". *Chemical Communications*, Vol. 53, n. 57, p. 8006-8009.
- West, A. C. 2013. "Electrochemistry and Electrochemical Engineering: An Introduction". Ed. Alan C. West, Columbia University, USA.
- Yan, X., Biemolt, J., Zhao, K., Zhao, Y., Cao, X., Yang, Y., and Yan, N. 2021. "A membrane-free flow electrolyzer operating at high current density using earth-abundant catalysts for water splitting". *Nature Communications*, Vol. 12, n. 1, p. 4143.
- Yang, G., Yu, S., Li, Y., Li, K., Ding, L., Xie, Z., and Zhang, F. Y. 2021. "A simple convertible electrolyzer in membraneless and membrane-based modes for understanding water splitting mechanism". *Journal of Power Sources*, Vol. 487, p. 229353.

7. RESPONSIBILITY NOTICE

The author(s) is (are) the only responsible for the printed material included in this paper.